Journal Pre-proof

Evaluation of *Vitis vinifera* seed oil as a green corrosion inhibitor for high-carbon steel and ferrovanadium alloys in sulfuric acid

Roland Tolulope Loto, Ordinakachukwu Uvemena Uyanwune, Ayomide Oreoluwa Oluwasesan, Ipinnuoluwa Joseph Oladipo, Marshal Emokpare Agbi

PII: S1452-3981(25)00011-2

DOI: https://doi.org/10.1016/j.ijoes.2025.100936

Reference: IJOES100936

To appear in: *International Journal of Electrochemical Science*

Received date: 18 December 2024
Revised date: 7 January 2025
Accepted date: 7 January 2025

Please cite this article as: Roland Tolulope Loto, Ordinakachukwu Uvemena Uyanwune, Ayomide Oreoluwa Oluwasesan, Ipinnuoluwa Joseph Oladipo and Marshal Emokpare Agbi, Evaluation of *Vitis vinifera* seed oil as a green corrosion inhibitor for high-carbon steel and ferrovanadium alloys in sulfuric acid, *International Journal of Electrochemical Science,* (2025) doi:https://doi.org/10.1016/j.ijoes.2025.100936

Evaluation of *Vitis vinifera* seed oil as a green corrosion inhibitor for high-carbon steel and ferrovanadium alloys in sulfuric acid

Roland Tolulope Loto[1]*, Ordinakachukwu Uvemena Uyanwune[1], Ayomide Oreoluwa Oluwasesan[1], Ipinnuoluwa Joseph Oladipo[1] and Marshal Emokpare Agbi[1]

[*1]Department of Mechanical Engineering, Covenant University, Ota, Ogun State, Nigeria
*tolu.loto@gmail.com

Abstract

The corrosion inhibition performance of *Vitis vinifera* seed oil (VVSO) was investigated on high-carbon steel (HCS) and ferrovanadium (FV) alloy in 0.25 M H_2SO_4 solution using gravimetric, potentiodynamic polarization, open circuit potential (OCP) measurements and optical microscopy. Gravimetric studies revealed superior inhibition efficiency on HCS, where corrosion rates decreased progressively with increasing VVSO concentration, reaching 95% efficiency at 0.5% VVSO after 360 hours of exposure. In comparison, FV alloys exhibited moderate inhibition, peaking at 73.95% at 2% VVSO. Potentiodynamic polarization results confirmed mixed-type inhibition behavior, with significant reductions in corrosion current density for HCS, correlating with efficiencies exceeding 70%. Conversely, for FV alloys, the highest inhibition efficiency of 72.95% was recorded at 2% VVSO, suggesting adsorption saturation at higher concentrations. Open circuit potential studies highlighted shifts to less negative potentials, indicative of enhanced corrosion resistance. For HCS, stabilization occurred around -0.490 V at 0.5% VVSO, forming a protective layer, while for FV, the potential stabilized at -0.495 V at 3% VVSO, demonstrating uniform inhibitor adsorption and reduced anodic dissolution. Overall, VVSO demonstrated concentration-dependent inhibition, exhibiting superior protection on HCS and moderate efficacy on FV as evident in the difference between the optical images of the inhibited and non-inhibited alloy surfaces. The findings underscore the potential of VVSO as an eco-friendly and effective corrosion inhibitor, with optimal performance influenced by substrate material and inhibitor concentration.

Keywords: corrosion; inhibitor; green compounds; steel; acid

1. Introduction

Corrosion poses a significant challenge in industrial applications, particularly in aqueous environments containing aggressive anions such as Cl^-, SO_4^{2-}, Br^-, NO_3^-, and OH^- [1]. Carbon steel, valued for its cost-effectiveness and favorable mechanical properties, is especially susceptible to degradation in such environments. Accounting for the majority of global steel production, carbon steel finds extensive applications in construction, pipelines, machinery, and chemical processing equipment [2,3]. However, its vulnerability to corrosion in acidic environments, including those involving sulphuric acid, results in substantial economic losses and safety concerns. Global studies estimate that corrosion incurs annual losses amounting to billions of dollars, with a considerable proportion attributed to carbon steel degradation [4, 5]. Industries reliant on sulphuric acid as a critical intermediate face persistent challenges, such as frequent maintenance and replacement of corroded components, operational inefficiencies due to downtime, and increased environmental risks associated with leaks and failures [6, 7]. These issues underscore the necessity of developing cost-effective and sustainable corrosion mitigation strategies to enhance the longevity and reliability of carbon steel infrastructure.

Traditional corrosion inhibitors, such as chromates, phosphates, and amines, have been widely employed to mitigate corrosion. While these inhibitors demonstrate high efficacy in reducing corrosion rates, they present substantial drawbacks, including environmental toxicity, health hazards, and economic constraints [8, 9]. Their use often necessitates complex monitoring and waste management systems, which further escalate operational costs. Moreover, regulatory pressures and rising environmental awareness have intensified the demand for environmentally benign alternatives. Green corrosion inhibitors represent a sustainable alternative to conventional inhibitors. Derived from natural sources such as plant extracts, biopolymers, and essential oils, these inhibitors achieve comparable performance while significantly minimizing environmental impact [10, 11]. Mechanistically, green inhibitors function by adsorbing onto metal surfaces, forming a protective barrier that limits direct exposure to the corrosive medium. The adsorption mechanisms are primarily categorized into physisorption and chemisorption. The efficacy of green inhibitors is influenced by factors such as molecular structure, concentration, and the nature of interactions with the metal surface [12]. Research highlights that compounds containing heteroatoms such as nitrogen, oxygen, and sulfur exhibit superior adsorption efficiency due to their

ability to donate electron pairs to the metal surface, thereby enhancing the protective barrier [13, 14].

Transition from laboratory research to industrial-scale application of green inhibitors is not without challenges. Key considerations include quality and consistency, optimization and system compatibility. The corrosion inhibitor industry is witnessing a paradigm shift towards sustainability and multifunctionality. Key developments include multifunctional Inhibitors, advanced characterization techniques, nanotechnology Integration, and regulatory and policy support. The future of corrosion management hinges on the systematic exploration and documentation of natural extracts with corrosion inhibition properties [15, 16]. Establishing a comprehensive repository of effective inhibitors will facilitate their widespread adoption and drive innovation in sustainable practices. Furthermore, interdisciplinary collaboration among materials scientists, chemists, and engineers will be instrumental in overcoming scalability and economic challenges.

Corrosion of carbon steel in aggressive environments remains a significant challenge across industries, contributing to economic losses and environmental risks [17-19]. While traditional inhibitors have provided effective solutions, their environmental and economic limitations underscore the necessity of transitioning to sustainable alternatives. Green corrosion inhibitors, derived from renewable natural compounds, represent a promising avenue that aligns with global efforts to mitigate industrial pollution and promote sustainability [20-22]. By prioritizing research, innovation, and sustainability, the corrosion inhibitor industry can achieve long-term solutions that protect critical infrastructure while safeguarding environmental health. In contribution to the research on corrosion inhibitors from natural extract. This manuscript focusses on the corrosion inhibition properties of grapeseed essential on high carbon steel and ferrovanadium alloy in dilute sulphuric acid.

2. Experimental methods

2.1 Materials and preparation

High carbon steel (HCS) and ferrovanadium alloy (FV) specimens obtained from automobile scrap was characterized with PhenomWorld scanning electron microscope at the Materials

Characterization Laboratory at Mechanical Engineering Department, Ota, Ogun State, Nigeria. The nominal (wt. %) content of HCS and FV are depicted in Table 1. The HCS and FV specimens were cut to average dimensions of 1 cm x 1cm x 0.5 cm (length, breadth and thickness) before embedding in resin mounts. The exposed surface of the steel was grinded with grinding papers (80, 320, 600, 800 and 1000 grits) and polished with 6 µm diamond polishing paste before cleaning with distilled water and acetone. Vitis Vinifera Seed Oil (VVSO) was purchased from Elsie Organics, Nigeria was prepared in volumetric concentrations of 0%, 0.5%, 1%, 1.5%, 2%, 2.5% and 3% respectively per 200 mL of 0.25 M H_2SO_4 acid solutions.

Table 1: Composition (wt. %) of HCS and FV

HCS										
Element Symbol	Al	Cr	Cu	C	Mn	P	S	Cs	V	Fe
Composition (wt. %)	0.0600	0.15	0.1	3.40	0.2	0.01	0.001	-	0.07	96.01
FV										
Element Symbol	Al	Cr	Cu	C	Mn	P	S	Cs	V	Fe
Composition (wt. %)	-	-	-	0.24	-	-	-	4.48	17.86	77.42

2.2 Potentiodynamic polarization test and open circuit potential measurement

Application of electrochemical methods through potentiodynamic polarization and potential-time measurement was done at 30 ˚C for 30 mins with a ternary multicomponent electrode system. They consist of resin mounted HCS and FV working electrodes with exposed surface area of 1 cm^3, Ag/AgCl reference electrode and platinum counter electrode within a transparent glass cell containing 200 mL of the acid/inhibitor electrolyte solution at predetermined VVSO concentrations interfaced with Digi-Ivy 2311 potentiostat and computer. Polarization plots were produced at a scan rate of 0.001 V/s in between potentials of -1 V and +1.5 V. Corrosion current density C_J, (A/cm^2) and corrosion potential, C_p (V) values were determined by Tafel extrapolation method whereby the estimated corrosion current, C_I (A) was obtained from the intercept of the two linear segment of the Tafel slope from the cathodic and anodic polarization plots. Corrosion rate, C_R (mm/y) was determined from the mathematical relationship;

$$C_R = \frac{0.00327 \times C_J \times E_{qv}}{d} \quad (1)$$

where E_{qv} is the equivalent weight (g) of metal, 0.00327 is a constant for corrosion rate calculation and d is the density (g/cm^3). The inhibition efficiency, ξ_F (%) was determined from the corrosion rate values according to equation 2;

$$\xi_F = \left[1 - \left(\frac{C_{R2}}{C_{R1}}\right)\right] \times 100 \quad (2)$$

C_{R1} and C_{R2} are the weight loss without and with VVSO inhibitor. Open-circuit potential (OCP) measurements were conducted at a step potential of 0.1 V/s over a duration of 5400 seconds in a 0.25 M H_2SO_4 solution containing VVSO concentrations of 0%, 0.5% and 3%. The experimental setup included a silver/silver chloride (Ag/AgCl) reference electrode and a resin-mounted steel working electrode immersed in 200 mL of the acid-chloride solution. The system was interfaced with a Digi-Ivy 2311 potentiostat and a computer for data acquisition and analysis.

2.3 Weight loss measurement and optical microscopy characterization

Measured MS steel coupons separately suspended in 200 mL of the dilute acid test solution for 360 h at 30 ^oC were weighed every 24 h. Corrosion rate, C_R (mm/y) was determined as follows;

$$C_R = \left[\frac{87.6\omega}{DAt}\right] \quad (4)$$

ω is the weight loss (g), D is the density (g/cm^3), A is the total surface area of the coupon (cm^2) and 87.6 is a constant for corrosion rate determination. t is the time (h). Inhibition efficiency (η) was determined from the mathematical relationship;

$$\eta = \left[\frac{\omega_1 - \omega_2}{\omega_1}\right] \times 100 \quad (5)$$

ω_1 and ω_2 are the weight loss at specific VVSO concentrations. Optical macro -images of corroded and inhibited HCS and FV morphology were analyzed after corrosion test with USB digital microscope.

3. Results and discussion

3.1 Gravimetric studies

Corrosion of HCS and FV alloys in 0.25 M H_2SO_4 solution at 0% to 3% VVSO concentration was studied for 360 h by gravimetric method. The plot of HCS and FV corrosion rate versus exposure time are shown in Fig. 1a and b while Fig. 2a and b shows the plot of VVSO inhibition efficiency versus exposure time for HCS and FV. Table 2 shows the gravimetric data of both alloys at 360 h of exposure. FV alloy exhibited significantly higher corrosion rate values throughout the exposure hours compared to HCS. Corrosion rate for FV alloy initiated (24 hours) at maximum value of 125.29 mm/y at 0% VVSO and minimum of 68.91 mm/y at 1% VVSO concentration. FV corrosion rate generally decreased in a parabolic manner with exposure time culminating (360 hours) at

values between 33.6 mm/y at 0% VVSO, and 8.75 mm/y at 2% VVSO concentration. The corresponding corrosion rate values for HCS shows HCS is significantly more corrosion resistant than FV with and without the presence of VVSO corrosion inhibitor compound. At 0% VVSO concentration and 24 hours of exposure, corrosion rate of HCS initiated at 22.76 mm/y compared to 125.22 for FV alloy. Corrosion of HCS at 0% VVSO concentration decreased to 14.23 mm/y at 360 hours of exposure compared to 33.6 mm/y for FV alloy. At 0.5% to 3% VVSO concentration, Corrosion rate of HCS varied at values between 13.11 mm/y at 0.5% VVSO and 9.84 mm/y at 3% VVSO concentration at 24 hours. At 360 h of exposure, the values have decreased to 0.71 mm/y (0.5% VVSO) and 0.99 mm/y (3% VVSO concentration). This shows VVSO inhibitor performed more effectively on HCS than FV.

Comparing the plot of inhibition efficiency versus exposure time for VVSO inhibition performance on FV and HCS alloys shows VVSO effectively inhibited HCS corrosion compared to FV. VVSO inhibition on FV initiated (24 hours) at values of 9.31%, 44.96%, 43.99%, 43.35%, 44.83% and 20.96% at 0.5% to 3% VVSO concentration. These values decreased to 0.80%, 14.21%, 7.56%, 19.89%, 1.93% and 12.06% at 120 hours of exposure. Beyond 120 hours' inhibition efficiency increased to final values of 73.84%, 73.42%, 72.27%, 73.95%, 71.31% and 70.13% at 360 hours of exposure. These observation shows that VVSO inhibition performance on FV is significantly dependent on time and less dependent on its concentration. Inhibition efficiency of VVSO on HCS initiated (24 hours) values of 42.38%, 31.52%, 48.81%, 45.14%, 50.47% and 56.75% (0.5% to 3% VVSO concentration). These values are comparable to the initial values for FV with the exception of FV value at 0.5% and 3% VVSO concentration. VVSO inhibition values for HCS generally increased progressively with respect to exposure time attaining optimal values of 95.00%, 92.20%, 91.85%, 93.96%, 94.84% and 93.01% at 360 hours of exposure. These values also show VVSO inhibition performance on HCS is significantly dependent on time and very much less on its concentration. However, the progressive increase in inhibition efficiency varies from the observation for FV alloy where the inhibition efficiency values increased and decreased before consistently increasing after 120 hours of exposure.

Table 2 Gravimetric data HCS and FV alloys at 360 h of exposure

HCS

VVSO Concentration (%)	Weight Loss (mg)	Corrosion Rate (mm/y)	Inhibition Efficiency (%)
0	2.479	14.228	-
0.5	0.124	0.711	95
1	0.193	1.11	92.2
1.5	0.202	1.16	91.85
2	0.15	0.859	93.96
2.5	0.128	0.734	94.84
3	0.173	0.994	93.01
FV			
VVSO Concentration (%)	**Weight Loss (mg)**	**Corrosion Rate (mm/y)**	**Inhibition Efficiency (%)**
0	3.274	33.601	-
0.5	0.856	8.789	73.84
1	0.870	8.930	73.42
1.5	0.908	9.317	72.27
2	0.853	8.752	73.95
2.5	0.939	9.640	71.31
3	0.978	10.035	70.13

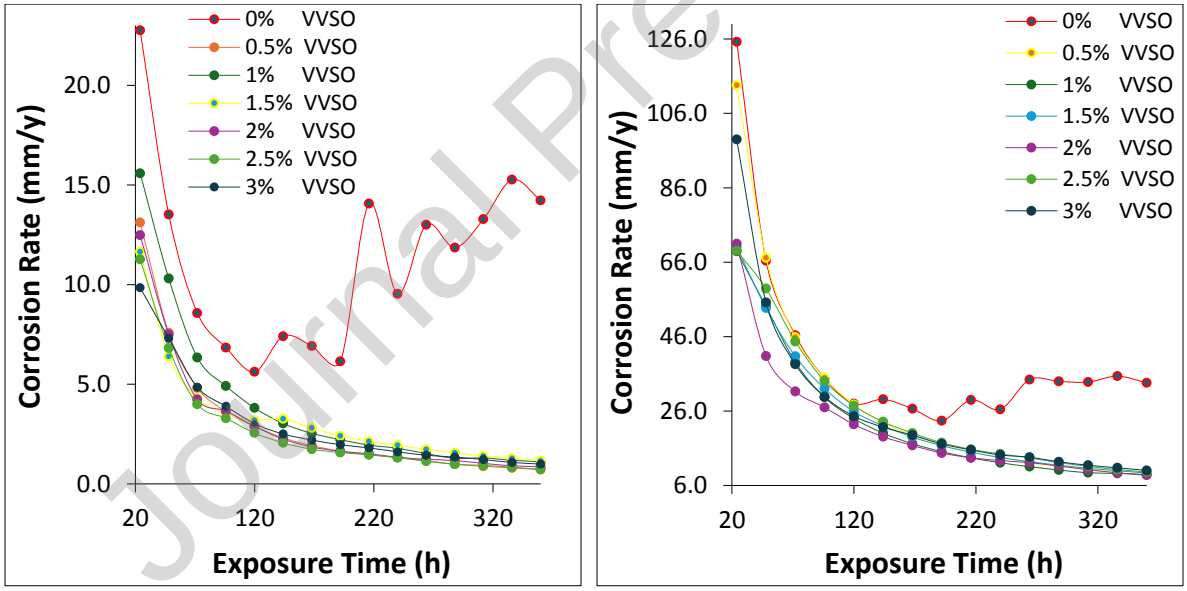

(a) (b)

Fig. 1 Plots of corrosion rate versus exposure time for (a) HCS and (b) FV in 0.25 M H_2SO_4 solution at 0% - 3% VVSO inhibitor concentration

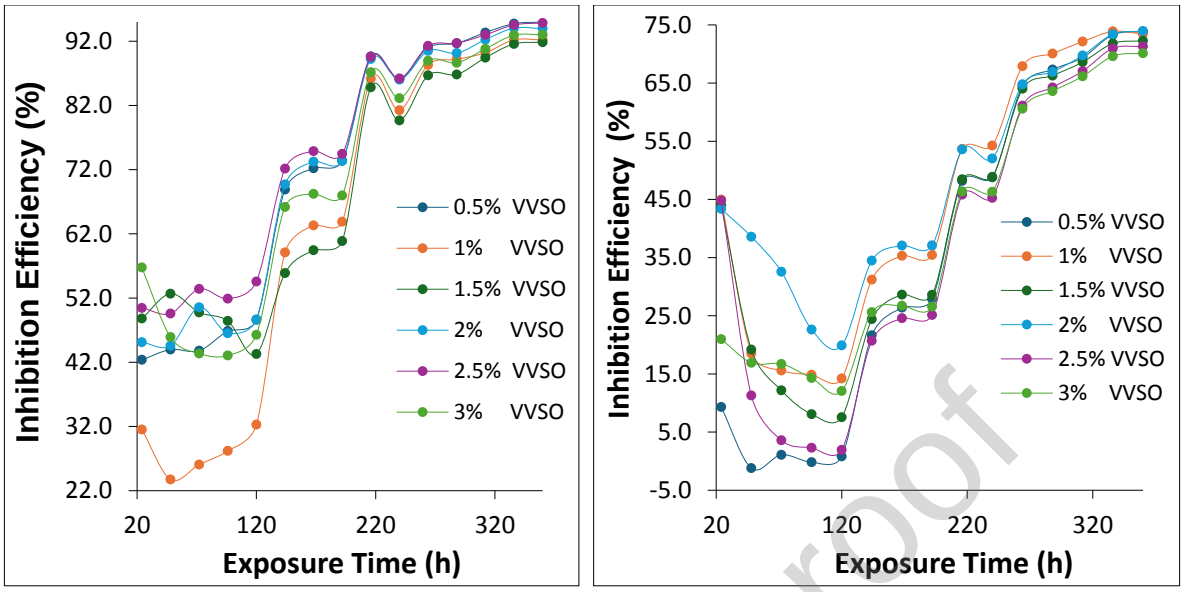

(a) (b)

Fig. 2 Plots of inhibition efficiency versus exposure time for (a) HCS and (b) FV in 0.25 M H_2SO_4 solution at 0% - 3% VVSO inhibitor concentration

3.2 Potentiodynamic polarization studies

Potentiodynamic polarization studies of VVSO inhibition performance on HCS and FV corrosion in 0.25 M H_2SO_4 solution are shown in Fig. 3a and b. Table 3 shows the potentiodynamic polarization data from the plots. The data in Table 3 shows VVSO performed more effectively on HCS than FV to a lesser degree compared to results from gravimetric analysis. At 0% VVSO concentration, HCS exhibited a corrosion rate value of 0.74 mm/y which corresponds to polarization resistance value of 5.51 Ω and corrosion current density of 6.07 x 10^{-3} A/cm^2. In the presence of VVSO compound at 0.5% concentration, HCS corrosion rate decreased to 0.244 mm/y corresponding to inhibition value of 67.03%, while at 3% concentration, the corrosion rate value is 0.171 mm/y corresponding to inhibition value of 76.91%. Observation of the inhibition value shows that beyond 0.5% VVSO concentration, VVSO inhibition value exceeded 70% inhibition unto 3% VVSO concentration. Secondly, increase in inhibition efficiency was progressive with respect to VVSO concentration. However, the increase is minimal. FV exhibited a corrosion rate of 0.104 mm/y at 0% VVSO concentration corresponding to corrosion current density of 8.49 x 10^{-4} A/cm^2 and polarization resistance of 21.56 Ω. The corrosion rate value decreased to 0.088 mm/y in the presence of 0.5% VVSO concentration corresponding to inhibition efficiency of 15.10%. Corrosion rate progressively decreased 0.028 mm/y at 2% VVSO concentration, corresponding to VVSO inhibition efficiency of 72.95%. This value is the peak value for VVSO

inhibition performance. Beyond 2% VVSO concentration, corrosion rate increased marginally while inhibition efficiency marginally decreased attaining inhibition value of 70.83% at 3% VVSO concentration.

Observation of the corrosion potential values on Fig. 3a and b shows shift in values in anodic and cathodic directions. However, the potential shift is below 85mV in either direction with respect to the potential values of HCS and FV at 0% VVSO concentration [23]. Hence VVSO inhibition behavior indicates mixed type inhibition action. The slope of the cathodic polarization in Fig. 3a curve indicates the charge transfer kinetics at the electrode interface. There configuration with respect to inhibitor concentration are similar indicating the mechanism of the cathodic reaction i.e. H_2 evolution and O_2 reduction remains unchanged [24, 25]. There is the possibility that VVSO inhibitor modified the corrosive solution and reduced the active sites for corrosion on HCS. The adsorption of the inhibitor follows a uniform mode from observation of the slopes indicating no significant change in the activation energy or transfer coefficient of the cathodic reaction [26, 27]. The anodic slope on the polarization plots for HCS, and the anodic/cathodic polarization plots for FV vary significantly with VVSO concentration indicating that the VVSO inhibitor alters the reaction pathway and creates a diffusion barrier for reactants. This is due to the influence of VVSO on the reaction kinetics occurring over the alloy surface.

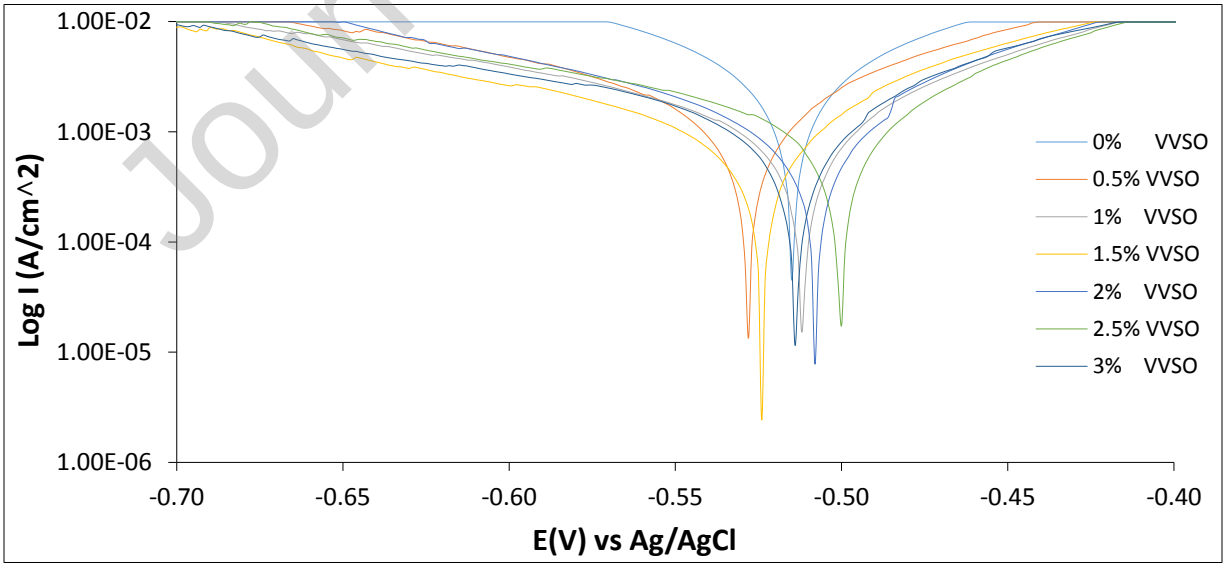

(a)

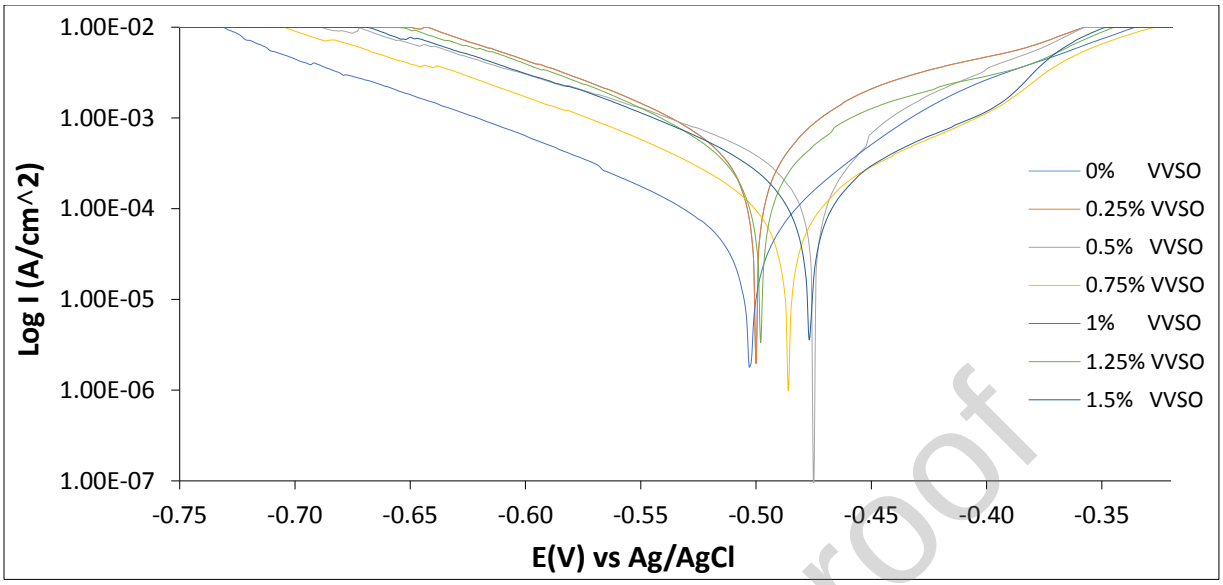

(b)

Fig. 3 Potentiodynamic polarization plots for (a) HCS and (b) FV in 0.25 M H_2SO_4 solution at 0% - 3% VVSO inhibitor concentration

Table 3 Potentiodynamic polarization data for HCS and FV alloys

HCS							
Sample	**VVSO Conc. (%)**	**Corrosion Rate (mm/y)**	**Inhibition efficiency (%)**	**Corrosion Current (A)**	**Corrosion Current Density (A/cm^2)**	**Corrosion Potential (V)**	**Polarization Resistance, *Rp* (Ω)**
A	0	0.740	-	6.07E-03	6.07E-03	-0.526	5.51
B	0.5	0.244	67.03	2.00E-03	2.00E-03	-0.528	12.84
C	1	0.180	75.71	1.47E-03	1.47E-03	-0.512	17.43
D	1.5	0.177	76.04	1.45E-03	1.45E-03	-0.524	17.53
E	2	0.176	76.27	1.44E-03	1.44E-03	-0.508	17.97
F	2.5	0.173	76.60	1.42E-03	1.42E-03	-0.500	18.14
G	3	0.171	76.91	1.40E-03	1.40E-03	-0.514	18.43
FV							
Sample	**VVSO Conc. (%)**	**Corrosion Rate (mm/y)**	**Inhibition efficiency (%)**	**Corrosion Current (A)**	**Corrosion Current Density (A/cm^2)**	**Corrosion Potential (V)**	**Polarization Resistance, *Rp* (Ω)**
A	0	0.104	-	8.49E-04	8.49E-04	-0.506	21.56
B	0.5	0.088	15.10	7.24E-04	7.24E-04	-0.500	65.48
C	1	0.057	45.14	4.68E-04	4.68E-04	-0.415	84.92
D	1.5	0.033	68.24	2.71E-04	2.71E-04	-0.486	143.60
E	2	0.028	72.95	2.31E-04	2.31E-04	-0.503	255.10
F	2.5	0.031	70.49	2.52E-04	2.52E-04	-0.498	138.69
G	3	0.030	70.83	2.49E-04	2.49E-04	-0.477	135.23

3.3 Open circuit potential measurement

The open circuit potential (OCP) plots for High Carbon Steel (HCS) and FV alloys in 0.25 M H_2SO_4 solution at 0%, 0.5%, and 3% VVSO inhibitor concentrations are presented in Fig. 4a and 4b. At 0% VVSO concentration, the OCP plots exhibit the most cathodic values, indicating a high

susceptibility to corrosion. For HCS, the potential starts at -0.545 V (0 s) and increases parabolically to -0.510 V (1300 s), likely due to the formation of a porous oxide layer on the surface. This oxide does not provide significant corrosion protection but modifies the electrochemical reaction mechanism, as evidenced by the subsequent gradual increase to -0.501 V (5400 s) [28]. The slow upward trend suggests minor surface stabilization, but the steel remains highly active to corrosion. In comparison, the FV alloy at 0% VVSO begins at a more positive potential (-0.512 V) and stabilizes quickly at -0.492 V (5400 s), reflecting greater thermodynamic stability and superior corrosion resistance relative to HCS [29, 30].

At 0.5% and 3% VVSO concentrations, significant shifts to less negative potentials are observed, signifying improved corrosion resistance. This improvement is attributed to the adsorption of VVSO molecules, which mitigate the aggressive action of SO_4^{2-} ions. For HCS, the OCP at 0.5% VVSO stabilizes around -0.490 V, indicating effective inhibition and a more stable, protective film after ~1000 s. However, at 3% VVSO, the potential becomes slightly less positive compared to 0.5%, suggesting possible saturation of adsorption sites or partial desorption of inhibitor molecules. Whereas for the FV alloy, the OCP behavior at 0.5% and 3% VVSO concentrations demonstrates greater corrosion resistance compared to HCS. The initial potential for FV at 0.5% starts at -0.461 V and stabilizes at -0.465 V (5400 s), whereas at 3% VVSO, the potential stabilizes around -0.495 V. The lack of large fluctuations at higher concentrations indicates the formation of a uniform, protective inhibitor layer, reducing the anodic dissolution rate [31, 32].

0.5% VVSO demonstrates optimal performance for HCS, with a consistently higher and more stable potential, reducing active corrosion sites via VVSO adsorption. while the FV alloy, 3% VVSO concentration provides the most effective protection, as indicated by the more stable and less fluctuating OCP profile, reflecting uniform inhibitor coverage and enhanced resistance to corrosion. The observed fluctuations at 0.5% VVSO for both alloys may suggest localized corrosion events or incomplete inhibition. While 0.5% VVSO delivers optimal corrosion inhibition for HCS, the FV alloy exhibits superior performance at 3% VVSO, indicating a material-specific response to VVSO concentration. The trends suggest an optimal inhibitor concentration, beyond which further additions yield diminishing improvements due to surface saturation or competitive adsorption mechanisms [33, 34].

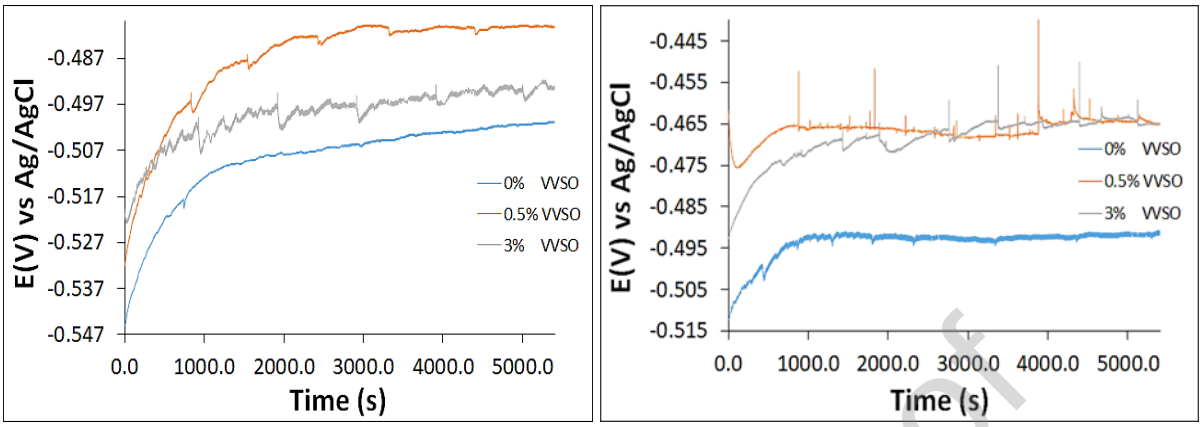

(a) (b)

Fig. 4 Open circuit potential plots of (a) HCS and (b) FV corrosion at 0%, 0.5% and 3% VVSO concentration with respect to exposure time

3.4 Optical microscopy studies

Optical images of HCS and FV are shown from Fig. 5a -g. Fig. 5a and b shows the etched optical images of HCS and FV before corrosion test. The images show slightly similar morphology due to the high Fe content. Fig. 5c and d shows the optical images after corrosion in 0.25 M H_2SO_4 solution without inhibitor addition. The images show a severely degraded morphology due to the electrochemical action of SO_4^{2-} ions. The ions oxidized the alloy surfaces resulting in corrosion of the alloys. The extent of deterioration slightly decreased in Fig. 5e and f due to the action of inhibitor molecules at 0.5% concentration which undoubtedly reduced the deteriorating effect of the SO_4^{2-} ions. Fig. 5g and h shows further decrease in surface deterioration due to the action of the inhibitor molecules at 3% concentration.

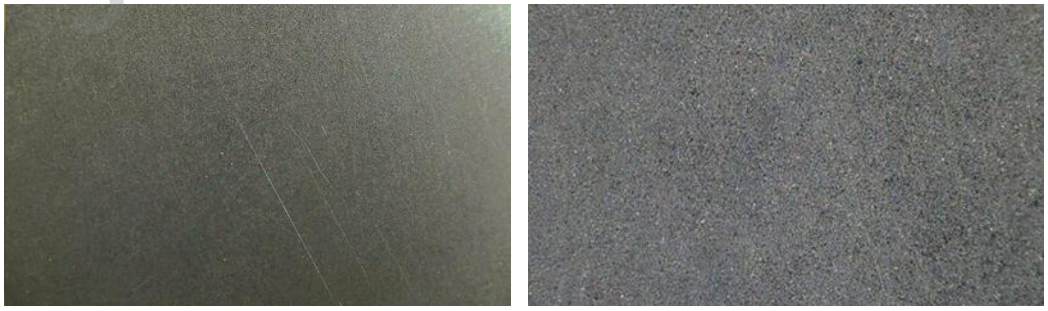

(a) (b)

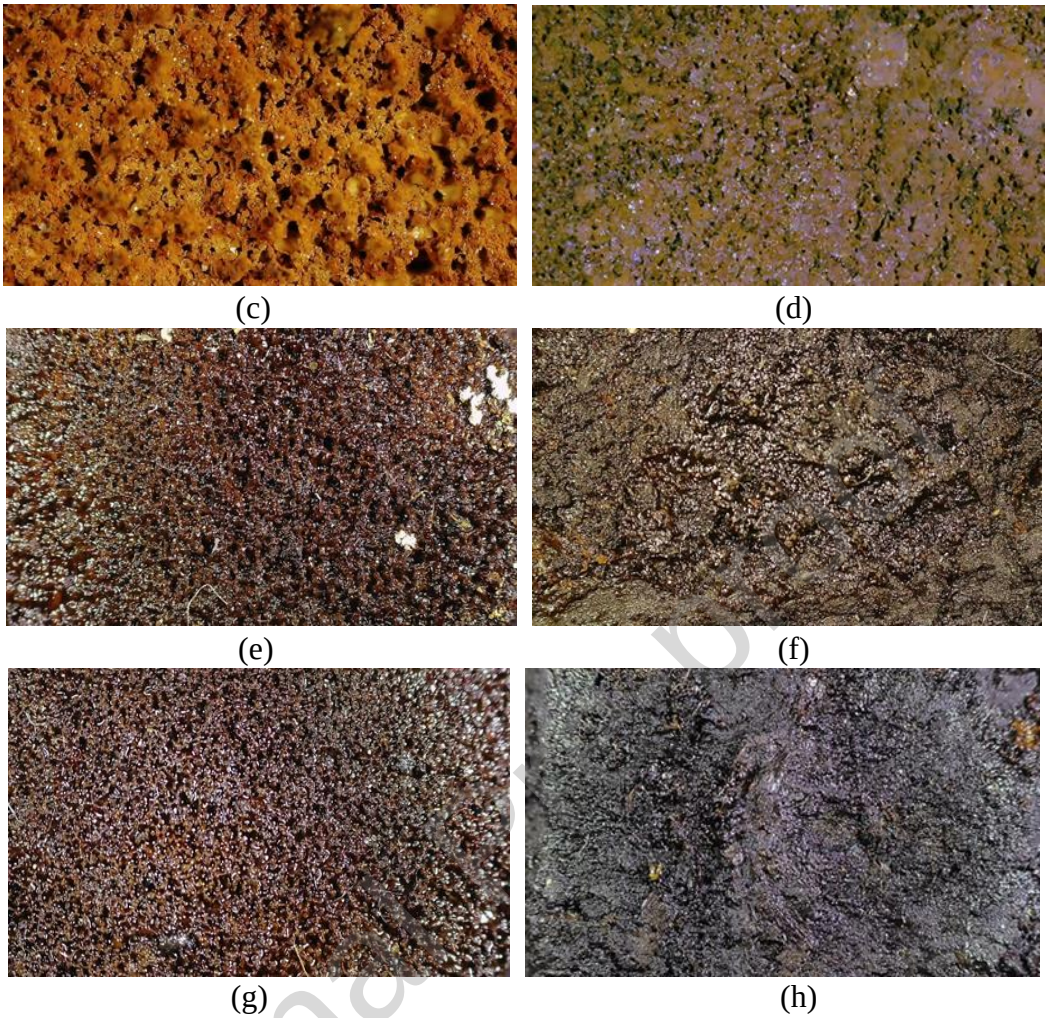

Fig. 5 Optical images of (a) and (b) etched HCS and FV surfaces, (c) and (d) corroded HCS and FV surfaces without VVSO inhibitor, (e) and (f) HCS and FV surfaces in 0.25 M H_2SO_4 with 0.5% VVSO inhibitor, and (g) and (h) HCS and FV surfaces in 0.25 M H_2SO_4 with 3% VVSO inhibitor

3.5 Comparison with literature

Rani and Selvaraj [35] studied the inhibitive action of vitis vinifera (grape) on copper and brass in natural sea water environment, Kaushik et al [36] studied the inhibitive action of grape seed extract as an environment-friendly green inhibitor for corrosion of mild steel in 1 M sulfamic acid, Batah et al [37] studied the corrosion inhibition effect of grape seed oil for corrosion inhibition using computational modeling techniques, and Bazgir [38] studied the corrosion mitigation of mild steel in hydrochloric acid solution using grape seed extract. Results show the grape seed oil/extract generally performed effectively with respect to concentration. Their mechanism of inhibition differs with respect to type of environment, type of alloy and concentration of inhibitor. Table 4

below shows the summary of comparative analysis of their results with VVSO inhibitor. Observation of the table shows VVSO extract performed more effectively on HCS in H_2SO_4 solution at 95% efficiency. This was followed by Vitis vinifera seed extract on brss in natural seawater at 92.29% efficiency. Grape seed extract also performed effectively on carbon steel in HCl solution according to the work of Marhamati et al [38] and Batah et al [37]. This shows the immense potential of VVSO inhibitor for corrosion prevention of metallic alloys. However, the performance of grapeseed oil on mild steel in sulfamic acid was marginal at 65% efficiency. According to the table, the inhibitor showed mixed type inhibition.

Table 4 Comparative summary of the corrosion inhibition properties of grape seed extracts

Author / **Criteria**	**Marhamati et al** [38]	**Batah et al** [37]	**Kaushik et al** [36]	**Rani and Selvaraj** [35]	**VVSO Inhibitor**
Inhibitor Used	Grape Seed Extract	Grape Seed Oil	Grape Seed Extract	Vitis vinifera seed & skin extract	Vitis vinifera seed oil (VVSO)
Medium	1 M HCl solution	1 M HCl solution	1 M Sulfamic acid	Natural sea water	0.25 M H_2SO_4
Inhibition Efficiency (Max)	>90% (300 ppm, chemisorption mechanism)	~90% (0.5 g/L)	65% (0.24 g/L)	92.29% for brass (1000 ppm); 76.08% for copper (303K)	HCS: 95% (0.5% VVSO, 360 h); FV: ~73% (2% VVSO, 360 h)
Mechanism	Mixed-type inhibitor; Horizontal molecule alignment	Synergistic adsorption (OA and LA molecules)	Mixed-type inhibitor	Adsorption through polyphenolic compounds	Mixed-type inhibitor; progressive adsorption with surface coverage
Substrate	Mild Steel	Carbon Steel (C38)	Mild Steel	Copper and Brass	High-Carbon Steel (HCS) and Ferrovanadium Alloys (FV)

3.6 Mechanism of Corrosion Inhibition by VVSO

The corrosion inhibition mechanism of VVSO on HCS and FV alloys in 0.25 M H_2SO_4 solution involves multiple interacting processes, primarily centered on the adsorption and protective layer formation on the metal surface. The inhibition properties of VVSO are rooted in its ability to adsorb onto the metal surface, forming a monolayer that blocks active corrosion sites. This adsorption process follows the Langmuir adsorption isotherm, suggesting a uniform monolayer coverage without significant lateral interaction among the adsorbed molecules. The adsorption is facilitated by the presence of functional groups such as hydroxyl (-OH) and carboxyl (-COOH) within VVSO, which interact with the metal surface by donating electrons to the empty d-orbitals

of the metal atoms, forming coordinate covalent bonds. This strong chemisorption ensures a stable and durable protective layer, critical for effective corrosion mitigation [39].

VVSO acts as a mixed-type inhibitor, targeting both anodic and cathodic reactions. This dual-action mechanism is evident from the potentiodynamic polarization studies. The inhibitor molecules align horizontally on the metal surface to maximize coverage. This orientation facilitates the formation of a uniform protective layer, enhancing the corrosion resistance. The inhibition efficiency of VVSO increases progressively with concentration, though it plateaus at higher concentrations (≥2%), likely due to surface saturation where additional VVSO molecules cannot effectively adsorb. The effectiveness of VVSO improves significantly over time. Gravimetric studies reveal that the inhibition efficiency for HCS increases from initial values of ~42-56% (depending on concentration) to 95% after 360 hours. This trend underscores the time-dependent stabilization of the protective layer, as VVSO molecules adsorb progressively and form a robust barrier against corrosion. The inhibition efficiency for FV alloys also improves with time, though it remains lower (~73%) compared to HCS, reflecting the material-specific nature of VVSO's performance. Optical microscopy provides visual evidence of VVSO's effectiveness. Before the addition of VVSO, severe degradation of the metal surface is observed due to the corrosive action of sulfate ions. However, with increasing VVSO concentrations, the surface morphology improves significantly, showing smoother and less corroded surfaces [40].

Conclusion

This study highlights the effectiveness of *Vitis vinifera* seed oil (VVSO) as an eco-friendly corrosion inhibitor for high-carbon steel (HCS) and ferrovanadium (FV) alloys in dilute sulfuric acid. Gravimetric analysis showed that VVSO achieved a maximum inhibition efficiency of 95% on HCS at 0.5% concentration, while FV alloys reached 73.95% efficiency at 2% VVSO. Potentiodynamic polarization confirmed VVSO's mixed-type inhibition behavior, significantly reducing corrosion rates for both alloys. Open circuit potential measurements revealed improved corrosion resistance, with HCS stabilizing at -0.490 V at 0.5% VVSO and FV stabilizing at -0.495 V at 3% VVSO. Overall, VVSO provided superior protection for HCS, while FV required higher concentrations for optimal performance. Optical images show the presence of the inhibitor limited the deterioration of the alloy surfaces compared to the non-inhibited alloy surfaces. These findings underscore VVSO's potential as a sustainable alternative to conventional inhibitors, offering

effective protection with minimal environmental impact. Future research should focus on optimizing VVSO for diverse materials and evaluating its long-term stability in industrial applications.

Acknowledgement

The author appreciates Covenant University for their financial support and provision of research facilities.

References

1. M. Vakili, P. Koutník, J. Kohout, Z. Gholami, Analysis, Assessment, and Mitigation of Stress Corrosion Cracking in Austenitic Stainless Steels in the Oil and Gas Sector: A Review. Surfaces. 7 (2024) 589-642. https://doi.org/10.3390/surfaces7030040.
2. S. Papavinasam, Chapter 3 - Materials, Corrosion Control in the Oil and Gas Industry, Gulf Professional Publishing, Houston, Texas, 2014, pp.133-177. https://doi.org/10.1016/B978-0-12-397022-0.00003-0.
3. K. Sotoodeh, Chapter Twelve - Material selection and corrosion, Subsea Valves and Actuators for the Oil and Gas Industry, Gulf Professional Publishing, Houston, Texas, 2021, pp.421-457. https://doi.org/10.1016/B978-0-323-90605-0.00004-9.
4. Z. May, M.K. Alam, N.A. Nayan, Recent advances in nondestructive method and assessment of corrosion undercoating in carbon–steel pipelines. Sensors, 22 (2022) 6654. https://doi.org/10.3390/s22176654.
5. L.T. Popoola, A.S. Grema, G.K. Latinwo, B. Gutti, A.S. Balogun, Corrosion problems during oil and gas production and its mitigation. Int. J. Ind. Chem. 4 (2013) 35. https://doi.org/10.1186/2228-5547-4-35.
6. A. Ouarga, T. Zirari, S. Fashu, M. Lahcini, H.B. Youcef, V. Trabadelo, Corrosion of iron and nickel-based alloys in sulphuric acid: Challenges and prevention strategies. J. Mater. Res. Technol. 26 (2023) 5105-5125. https://doi.org/10.1016/j.jmrt.2023.08.198.
7. M.S. Kim, J.A. Jeong, Corrosion behavior of carbon steel in diluted sulfuric acid based on seawater. Corros. Eng. Sci. Technol. 18(3) (2019) 78-85. https://doi.org/10.14773/cst.2019.18.3.78.

8. A.A. Al-Amiery, E. Yousif, W.N.R.W. Isahak, W.K. Al-Azzawi, A Review of Inorganic Corrosion Inhibitors: Types, Mechanisms, and Applications. Tribol. Ind. 45(2) (2022) 313-339. https://doi.org/10.24874/ti.1456.03.23.06.
9. S. Zehra, M. Mobin, J. Aslam, Chapter 13 - Chromates as corrosion inhibitors, in: C. Verma, J. Aslam, C. M. Hussain, Inorganic Anticorrosive Materials, Past, Present and Future Perspectives, Elsevier, Amsterdam, 2022, pp.251-268. https://doi.org/10.1016/B978-0-323-90410-0.00014-3.
10. H. Wei, B. Heidarshenas, L. Zhou, G. Hussain, Q. Li, K. Ostrikov, Green inhibitors for steel corrosion in acidic environment: state of art. Mater. Today Sustain. 10 (2020) 100044. https://doi.org/10.1016/j.mtsust.2020.100044.
11. N. Hossain, M.A. Chowdhury, M. Kchaou, An overview of green corrosion inhibitors for sustainable and environment friendly industrial development. J. Adhes. Sci. Technol. 35(7) (2020) 673-690. https://doi.org/10.1080/01694243.2020.1816793.
12. B.R. Holla, R. Mahesh, H.R. Manjunath, V.R. Anjanapura, Plant extracts as green corrosion inhibitors for different kinds of steel: A review. Heliyon. 10(14) (2024) e33748. https://doi.org/10.1016/j.heliyon.2024.e33748.
13. A. Thakur, A. Kumar, Sustainable Inhibitors for Corrosion Mitigation in Aggressive Corrosive Media: A Comprehensive Study. J. Bio Tribo Corros. 7 (2021) 67. https://doi.org/10.1007/s40735-021-00501-y.
14. L. Guo, I.B. Obot, X. Zheng, X. Shen, Y. Qiang, S. Kaya, C. Kaya, Theoretical insight into an empirical rule about organic corrosion inhibitors containing nitrogen, oxygen, and sulfur atoms. Appl. Surf. Sci. 406 (2017) 301-306. https://doi.org/10.1016/j.apsusc.2017.02.134.
15. S.Y. Begum, P.M. Imran, A. Kubaib, M.T. Yassin, F.O. Al-Otibi, M. Selvakumaran, A.A. Basha, S. Sulthanudeen, Unveiling multifunctional inhibitors: holistic spectral, electronic and molecular characterization, coupled with biological profiling of substituted pyridine derivatives against LD transpeptidase, heme oxygenase and PPAR gamma. RSC Adv. 14 (2024) 29896-29909. https://doi.org/10.1039/D4RA04217D.
16. C. Verma, E.E. Ebenso, M.A. Quraishi, C.M. Hussain, Recent developments in sustainable corrosion inhibitors: design, performance and industrial scale applications. Mater. Adv. 2 (2021) 3806-3850. https://doi.org/10.1039/D0MA00681E.

17. N. Timoudan, M. El Faydy, A. Titi, I. Warad, F. Benhiba, A. Alsulmi, B. Dikici, A. Touzani, A. Dafali, A. Bellaouchou, F. Bentiss, A. Zarrouk, Enhanced corrosion resistance of carbon steel in an aggressive environment by a recently developed pyrazole derivative: Electrochemical, SEM/XPS/AFM, and theoretical investigation. J. Solid State Electrochem. 28 (2024) 2837-2860. https://doi.org/10.1007/s10008-024-05846-1.
18. D. Dwivedi, K. Lepková, T. Becker, 2017. Carbon steel corrosion: a review of key surface properties and characterization methods. RSC Adv. 7 (2017) 4580-4610. https://doi.org/10.1039/C6RA25094G.
19. M. Tavakkolizadeh, H. Saadatmanesh, Galvanic corrosion of carbon and steel in aggressive environments. J. Compos. Constr. 5(3) (2001). https://doi.org/10.1061/(ASCE)1090-0268(2001)5:3(200).
20. R.T. Loto, O. Tiwa, Eugene, Synergistic combination effect of clove essential oil extract with basil and atlas cedar oil on the corrosion inhibition of low carbon steel. S. Afr. J. Chem. Eng. 30 (2019) 28-41. http://doi.org/10.1016/j.sajce.2019.08.001.
21. M.A. Fajobi, R.T. Loto, O.O. Oluwole, Corrosion in Crude Distillation Overhead System: A Review. J. Bio- Tribo-Corros. 5 (2019) 67. http://doi.org/10.1007/s40735-019-0262-4.
22. C.A. Loto, R.T. Loto, A.P.I. Popoola, Electrode potential monitoring of effect of plants extracts addition on the electrochemical corrosion behaviour of mild steel reinforcement in concrete. Int. J. Electochem. Sci. 6(8) 2011. http://doi.org/10.1016/s1452-3981(23)18264-2.
23. E.S. Ferreira, C. Giacomelli, F.C. Giacomelli, A. Spinelli, Evaluation of the inhibitor effect of L-ascorbic acid on the corrosion of mild steel. Mater. Chem. Phys. 83(1) (2004) 129-134. https://doi.org/10.1016/j.matchemphys.2003.09.020.
24. H. Ashassi-Sorkhabi, B. Shaabani, D. Seifzadeh, Corrosion inhibition of mild steel by some schiff base compounds in hydrochloric acid. Appl. Surf. Sci. 239(2) (2005) 154-164. https://doi.org/10.1016/j.apsusc.2004.05.143
25. M.A. Quraishi, D. Jamal, Fatty acid triazoles: Novel corrosion inhibitors for oil well steel (N-80) and mild steel. J. Amer. Oil Chem. Soc. 77 (2000) 1107-1111. https://doi.org/10.1007/s11746-000-0174-6.
26. A.K. Singh, S.K. Shukla, M.A. Quraishi, E.E. Ebenso, Investigation of adsorption characteristics of N, N'-methylimino-dimethylidyne-di-2,4-xylidine as corrosion inhibitor at

mild steel/sulphuric acid interface. J. Taiwan Inst. Chem. Eng. 43(3) (2012) 463-472. https://doi.org/10.1016/j.jtice.2011.10.012.

27. S.A. Soliman, M.S. Metwally, S. Selim, M.A. Bedair, M.A. Abbas, Corrosion inhibition and adsorption behavior of new Schiff base surfactant on steel in acidic environment: Experimental and theoretical studies. Ind. Eng. Chem. Res, 20(6) (2014) 4311-4320. https://doi.org/10.1016/j.jiec.2014.01.038.
28. K. Kim, Q.C. Sherman, L.K. Aagesen, P.W. Voorhees, Phase-field model of oxidation: Kinetics. Phys. Rev. E. 101 (2020) 022802. https://doi.org/10.1103/PhysRevE.101.022802.
29. X.G. Zhang, Corrosion Potential and Corrosion Current. In: Corrosion and Electrochemistry of Zinc. Springer, Boston, MA, 1996. https://doi.org/10.1007/978-1-4757-9877-7_5.
30. Y. Shi, B. Yang, P.K. Liaw, Corrosion-Resistant High-Entropy Alloys: A Review. Metals. 7 (2017) 43. https://doi.org/10.3390/met7020043.
31. Z. Zhang, F. Wang, Y. Liu, S. Wu, W. Li, W. Sun, D. Guo, J. Jiang, Molecule adsorption and corrosion mechanism of steel under protection of inhibitor in a simulated concrete solution with 3.5% NaCl. RSC Adv. 8 (2018) 20648-20654. https://doi.org/10.1039/C8RA03235A.
32. A. Chaouiki, M. Chafiq, Y.G. Ko, A.H. Al-Moubaraki, F.Z. Thari, R. Salghi, K. Karrouchi, K. Bougrin, I.H. Ali, H. Lgaz, Adsorption mechanism of eco-friendly corrosion inhibitors for exceptional corrosion protection of carbon steel: Electrochemical and first-principles DFT evaluations. Metals. 12 (2022) 1598. https://doi.org/10.3390/met12101598.
33. M.A. Migahed, M. Abd-El-Raouf, A.M. Al-Sabagh, H.M. Abd-El-Bary, Corrosion inhibition of carbon steel in acid chloride solution using ethoxylated fatty alkyl amine surfactants. J. Appl. Electrochem. 36 (2006) 395-402. https://doi.org/10.1007/s10800-005-9094-7.
34. L. Chen, D. Lu, Y. Zhang, Organic compounds as corrosion inhibitors for carbon steel in HCl solution: A comprehensive review. Materials. 15 (2023). https://doi.org/10.3390/ma15062023.
35. P. D. Rani, S. Selvaraj, Inhibitive action of vitis vinifera (grape) on copper and brass in natural sea water environment. Rasayan J. Chem. 3(3) (2010) 473-482.
36. N.P. Kaushik, P. Rao, N. Kedimar, A. S. A. Rao, Grape seed extract as an environment-friendly green inhibitor for corrosion of mild steel in 1 M sulfamic acid. J. of Materi. Eng & Perform. 33 (2024) 10885–10894. https://doi.org/10.1007/s11665-024-09802-y.

37. A. Batah, A. H. Al-Moubaraki, E. A. Noor, J. M. Al-Ahmari, A.A. Al-Ghamdi, O. I. El Mouden, R. Salghi, M. Chafiq, A. Chaouiki, Y. G. Ko, Environmentally benign grape seed oil for corrosion inhibition: cutting-edge computational modeling techniques revealing the intermolecular and intramolecular synergistic inhibition action. Coatings. 14 (2024) 77. https://doi.org/10.3390/coatings14010077.
38. F. Marhamati, M. Mahdavian, S. Bazgir, Corrosion mitigation of mild steel in hydrochloric acid solution using grape seed extract. Sci. Rep. 11 (2021) 18374. https://doi.org/10.1038/s41598-021-97944-7.
39. V. Saraswat, M. Yadav, I.B. Obot, Investigations on eco-friendly corrosion inhibitors for mild steel in acid environment: Electrochemical, DFT and Monte Carlo simulation approach. Colloids Surf. A Physicochem. Eng. Asp. 599 (2020) 124881.
40. O.M. Adesusi, O.R. Adetunji, T.J. Erinle, I.K. Okediran, O.O. Akinpelu, S.O. Ipadeola, Free fatty acid influenced corrosion inhibition mechanisms of some inedible plants seeds oils on low alloyed medium-carbon steel in H_2SO_4. World J. Eng. 19(4) (2022) 467-479. https://doi.org/10.1108/WJE-11-2020-0554.

Declaration of Competing Interest

The authors declare that they have no known competing financial interests or personal relationships that could have appeared to influence the work reported in this paper.